Nondestructive characterization of MOCVD-grown GaInAs/GaAs using rocking curve and topography

Chu R. Wie and H. M. Kim
State University of New York at Buffalo, Dept. of ECE, Amherst, NY 14260
K. M. Lau
University of Massachusetts, Dept. of ECE, Amherst, MA 01003

ABSTRACT

Partially relaxed GaInAs layers grown on (001) GaAs substrates by Metalorganic Chemical Vapor Deposition are studied using x-ray rocking curve (XRC) and double crystal topography, energy dispersive x-ray analysis (EDAX), and Nomarski phase contrast microscopy. Epilayers of 1 - 7 μm thickness are grown on various buffer layers. Epilayers grown on a plain GaAs buffer layer and on a graded GaInAs buffer layer contain many line defects (LD) and show cross-hatched patterns on the surface. The layer grown on a strained layer superlattice buffer layer is free of LD's and of the cross-hatched patterns. All the layers are relaxed by differing amounts along the two <110> directions. The XRC and EDAX measurements of the ternary layer compositions agree reasonably well. The mean spacing of misfit dislocations from XRC and the LD spacing from topography agree in the order of magnitude with the electron microscopy measurements by others. The XRC data on x-ray strain, elastic strain, and the misorientation angle between the epilayer and substrate are also presented.

1. INTRODUCTION

Lattice-mismatched strained $Ga_{1-x}In_xAs$/GaAs structures are becoming widely employed in devices because of the high electron mobility, and low bandgap which is advantageous for achieving additional band-edge discontinuities and for forming nonalloyed Ohmic contacts. Examples are the heterojunction bipolar transistor (HBT)[1], strained layer quantum well laser[2], and quantum well modulation doped field effect transistor (MODFET)[3]. Many device characteristics such as transconductance, maximum operating frequency, threshold current density, and low frequency noise are improved as a result of employing the GaInAs layer. Often, the GaInAs layer thickness exceeds the critical layer thickness and many misfit dislocations and other defects are generated at the interface and in the epi and buffer layers. Examples of devices employing the partially relaxed GaInAs layers are the HBT[4] and the nonalloyed Ohmic contact high electron mobility transistor (HEMT)[5]. In addition, the enhanced flexibility in bandgap engineering also motivates the use of partially relaxed epilayers.

The partially relaxed heterojunction epilayers contain many structural defects including misfit dislocation, threading dislocation, and dark line defects of unknown nature[6,4]. More detailed understanding of the microscopic structures of these defects and their effects to the electrical and optical properties is needed to determine the extent to which these structures can be employed in devices. Fitzgerald *et al.* studied the defect structures in the partially relaxed GaInAs layers and in the buffer layers using scanning cathodoluminescence (CL) and electron microscopy techniques[6]. They observed several different types of dislocations in the ternary epilayer and in the GaAs buffer layer. Ramberg *et al.* studied the performance of HBT's with partially relaxed GaInAs layers[4]. More studies along this line are needed. Correlation studies of the microstructural defects and the electrical effects for the partially relaxed samples are

particularly interesting for device applications.

The x-ray rocking curve and topographic studies are suitable in the correlation studies because of their nondestructive nature and yet providing many structural characteristics. The structural characteristics obtainable by XRC are the in-plane mismatch and average misfit dislocation spacings along the two <110> directions, the compressive, tensile and shear elastic strains in the epilayer, the crystallographic misorientation between the epilayer and the substrate, and the rocking curve width. Double crystal topography can provide images of the line defects in the epilayer, the local strain fields and their spatial variation. The spatial resolution of dark line defects is limited to about 1 μm. Many of the above parameters were measured for as-grown GaInAs epilayers[7], MeV ion-implanted bulk III-V's[8], MeV ion-implanted GaAs epilayers[9], and MeV ion-implanted GaInAs/GaAs samples[10]. The dynamical x-ray diffraction theory for application to rocking curve analysis is given in reference 11.

2. EXPERIMENTS AND RESULTS

Partially relaxed GaInAs single layers were grown on three different buffer layers (plain GaAs, graded GaInAs, and SLS) on (001) GaAs substrates whose surface normals are a few degrees off [001]. The samples were grown by metalorganic chemical vapor deposition (MOCVD) in a computer-controlled horizontal reactor system at atmospheric pressure and 650 °C. Trimethylgallium (TMG), trimethylindium (TMI) and 100 % AsH_3 were used as reactant sources. The TMG and TMI sources were held at -14 and 21 °C, respectively. The carrier gas was 8 slpm of palladium purified H_2. The TMG and TMI mole fractions were 5×10^{-5} and 1.25×10^{-5} respectively for the sample with a plain GaAs buffer. The indium composition and growth rate of the layers can be scaled linearly with the TMG and TMI mole fractions. Since the growth sequence was controlled with a microcomputer which operated the mass flow controllers and valves, the flow controllers for TMG and TMI were reset every 30 seconds with a 1-2 c.c./min change of the flow rate for the growth of the graded GaInAs buffer layer. For the SLS buffer, the TMI flow was removed periodically from the reaction chamber to obtain the alternating GaAs layer.

Samples were characterized by the double crystal x-ray rocking curve (XRC) technique, energy dispersive x-ray analysis (EDAX), double crystal topography (DCT), and the Nomarski phase contrast microscopy. The x-ray techniques are described below in detail.

2.1. Double crystal topography

A small incident angle 224 reflection of $CuK\alpha_1$ was used for the topography. A schematic diagram of the experimental setup is given in Figure 2(A). Before the topographic plate was placed to be exposed to the reflected x-ray beam, a rocking curve was taken and the sample goniometer was moved to an angle corresponding to the maximum slope of the epilayer peak as indicated in Figure 2(B). The scintillation detector was then replaced by an Ilford topographic plate with a 25 μm thick L-4 nuclear emulsion. The exposure time ranged from 30 minutes to several hours depending upon the reflected beam intensity. An optical micrograph was taken from the developed plate.

Topographic images of the epilayers of the three samples are given along with the Nomarski micrographs in Figure 1. The sample grown on a SLS buffer (Sample No.1)

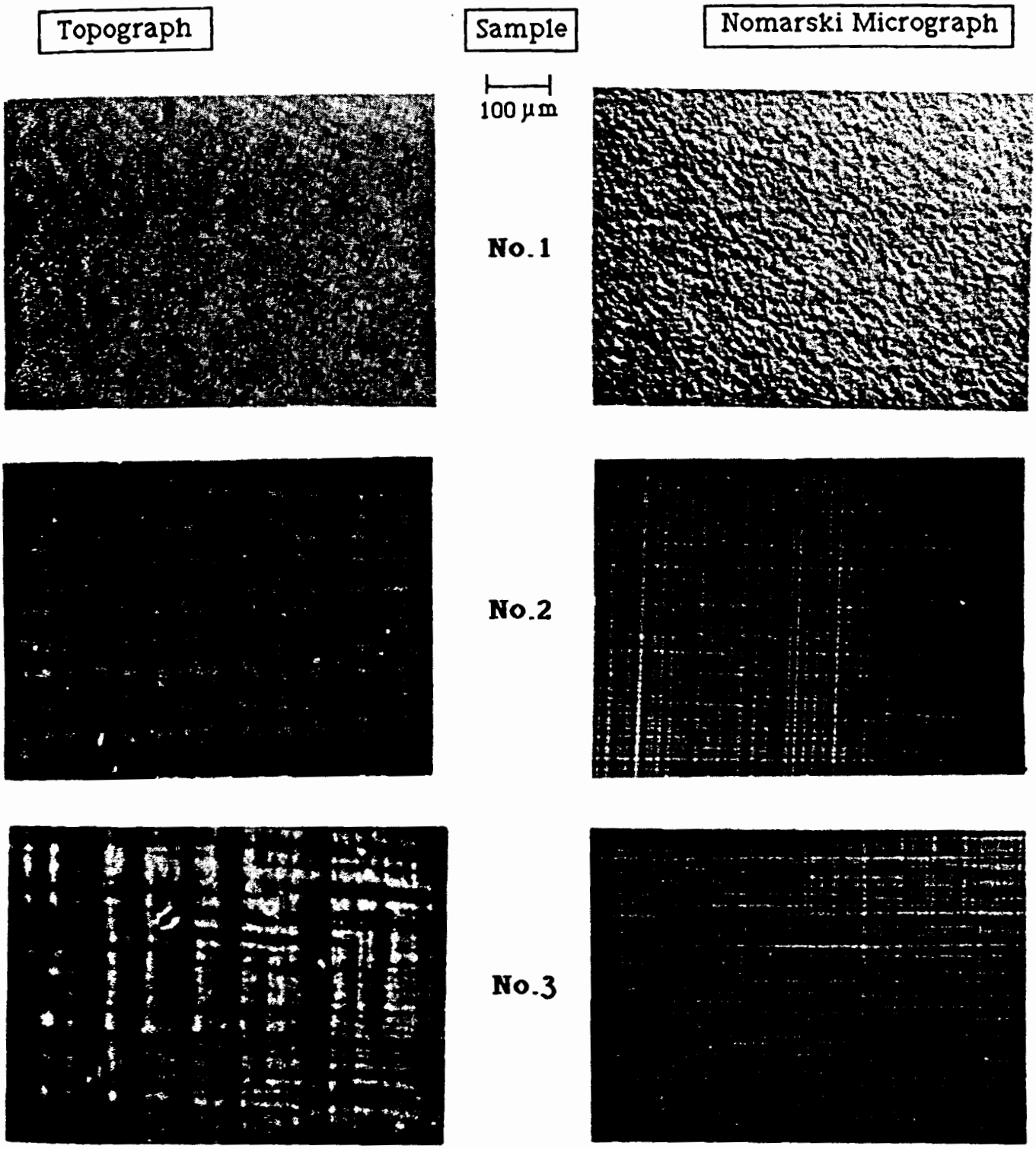

Figure 1. Double crystal topographs and Nomarski micrographs. Sample No.1 which has SLS buffer is free of line defects and surface ridges even if the elastic strain is comparable to other samples and it has a high density of threading dislocations (pits in Nomarski and black dots in topograph)

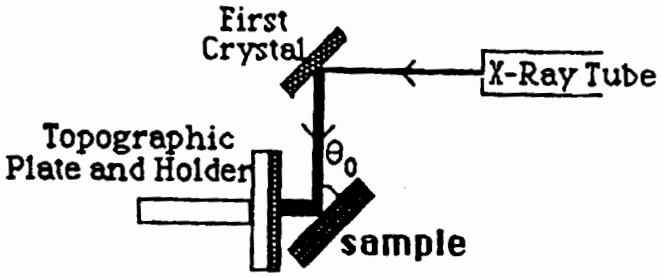

(A) Double crystal x-ray topography system. The angle θ_0 is marked in the rocking curve in next figure.

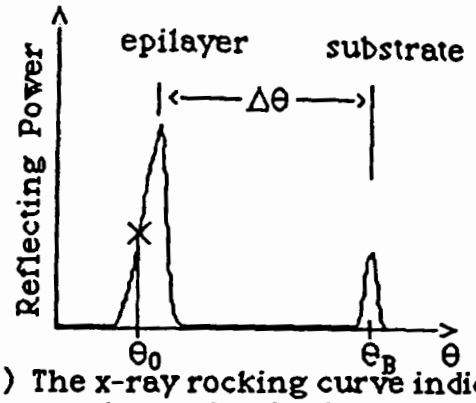

(B) The x-ray rocking curve indicates the angular setting in the topography. Causes for the angular separation are explained in Figures C, D, and G.

$$\Delta\theta = \Delta\theta_B + \Delta\psi \pm \Omega$$

$$\Delta\theta_B = -\frac{\Delta d}{d}\tan\theta_B = -(\sin^2\psi\ c^{xr}_{1\ or\ 2} + \cos^2\psi\ c^{xr}_3)\tan\theta_B$$

$$\Delta\psi = \pm \sin\psi\cos\psi\,(c^{xr}_{1\ or\ 2} - c^{xr}_3)$$

where,

$+ = \theta_B - \psi$ } incidence w.r.t.
$- = \theta_B + \psi$ } surface normal

(C) The three parts contributing to the angular separation between the epilayer and substrate peaks.

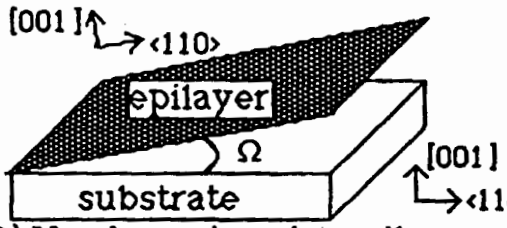

(D) Most heterojunction epilayers are slightly off-oriented from subtsrate. Ω = Misorientation angle.

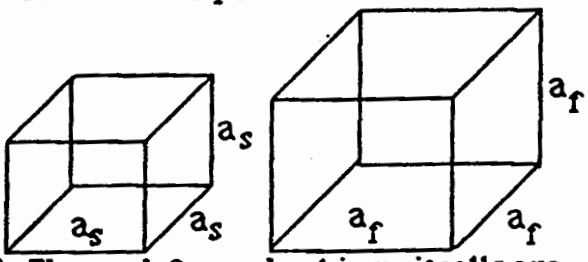

(E) The undeformed cubic unitcells are shown for the substrate and the epilayer.

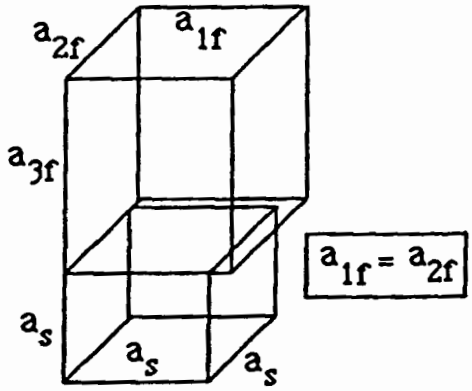

(F) Tetragonal distrotion of the epilayer.

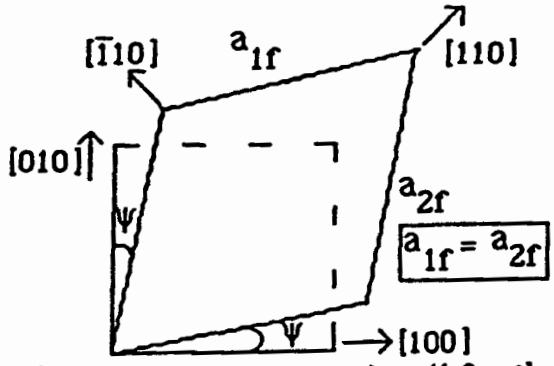

(H) Base plane of the unit cell for the epilayer is distorted due to unequal relaxation for the two <110> directions.

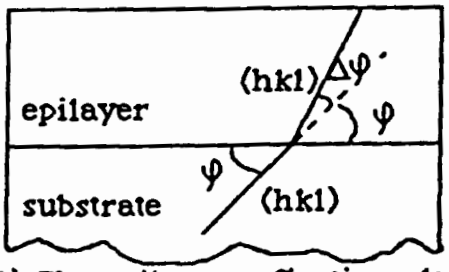

(G) The epilayer reflecting plane is at an angle $\Delta\psi$ with the substrate reflecting plane due to distortion.

Figure 2. The topography setup and the structural distortion of the epilayer.

shows no line defects or the cross-hatched patterns. Samples showing the line defects (LD) also show the cross-hatched patterns in the Nomarski micrographs. The layer grown on a graded GaInAs buffer layer (Sample No.2) does not show any distinct difference from the layer grown on a plain GaAs buffer (Sample No.3) in the LD density and in the surface morphology. . The LD spacings for both samples are roughly 5~10 μm. The uniformity and average density of these line defects are clearly different for the two <110> directions indicating an unequal relaxation along these two directions. This is verified by the different in-plane x-ray strains, ε_1^{xr} and ε_2^{xr}, in the XRC analysis. This also introduces an elastic shear strain in the (001) plane.

The line defects appear to develope before the lattice relaxation becomes measurable by the XRC technique[12]. However, the thickness of the samples studied here are all higher than the critical layer thickness. The electron microscopy studies show that the dislocation density is higher by about two orders of magnitude in a region near the interface than in a region which is away from the interface by more than 1 μm[6]. Consistent with this, the average spacing of misfit dislocations measured by XRC is 300~600 Å where as the line defect spacing is approximately 5~10 μm.

2.2 Double crystal x-ray rocking curve measurements

The XRC technique is described in reference 11. Briefly, the topographic plate in Figure 2(A) is replaced by the scintillation detector which counts the reflected beam intensity for a given amount of time at every step of the sample goniometer which rotates by a typical angular step of 0.001°. In the rocking curve (Figure 2(B)), the angular separation of the two peaks corresponding to the substrate and the epilayer respectively is composed of three parts: the Bragg angle difference ($\Delta\theta_B$) between the epilayer and substrate due to different d-spacing, the misorientation angle ($\Delta\varphi$) between the epilayer and substrate reflecting planes due to the tetragonal distortion of the epilayer unit cell, and the misorientation angle between the epilayer [001] direction and the substrate [001] direction which is present in almost all heterostructure samples arising from the epitaxial growth process. These terms are illustrated in Figures 2(B), 2(C), 2(D), 2(F) and 2(G). The misorientation angle between the epilayer [001] and substrate [001] was about 0.3° for the three samples (see Table 1).

The unit cell of a partially relaxed epilayer is shown in Figures 2(F) and 2(H). Parameters which are directly measured in the XRC are:

$$\varepsilon_n^{xr} = (d_{nf} - d_s)/d_s \qquad (1)$$

where n = 1, 2, or 3, corresponding to the two <110> in-plane directions and the [001] surface normal, respectively, and d_{nf} and d_s are the spacings of the reflecting lattice planes for the film and substrate in the three respective directions. The substrate unit cell is assumed to be an undistorted cubic cell. Here, ε_1^{xr} and ε_2^{xr} are the x-ray strains for the two <110> in-plane directions and ε_3^{xr} is the x-ray strain in direction normal to the surface. The two in-plane x-ray strains are directly related to the average spacings of misfit dislocations along each <110> in-plane direction by D= b/(2 $\varepsilon_{1 \text{ or } 2}^{xr}$), where b is the Burgers vector given by b=$a_s/\sqrt{2}$ and D is the spacing of 60° dislocations. When a SLS or graded buffer layer is present, for which the misfit dislocations may spread over many interfaces or over finite thickness, the above relation may apply to the average

Sample	Buffer & Thickness (μm)	Epilayer thickness (μm)	Composition "x" in the epilayer $Ga_{1-x}In_xAs$ (%)		Misfit, ε_f (%)	Average spacing of misfit disloc. (Å)		Misorientation, Ω (degree)
			XRC	EDAX		[110]	[$\bar{1}$10]	
No.1	SLS 0.8 μm	7.0 μm	5.6%	7.3%	0.401%	507 Å	668 Å	0.28°
No.2	Graded $Ga_{1-x}In_xAs$ $x=0\rightarrow0.13$ 4.5 μm	1.0 μm	13.3 %	13.8 %	0.953 %	234 Å	257 Å	0.35°
No.3	Plain GaAs 1.0 μm	4.0 μm	9.3 %	10.2 %	0.665 %	322 Å	345 Å	0.33°

Sample	X-ray strain (%)			Elastic strain (%)		
	ε_1^{xr} , [110]	ε_2^{xr} , [$\bar{1}$10]	ε_3^{xr} , [001]	ε_1 , [100] ε_2 , [010] Compressive	ε_3 , [001] Tensile	ε_6 , (001) Shear
No. 1	0.394 %	0.299 %	0.451 %	- 0.054 %	0.049 %	0.095 %
No.2	0.853 %	0.779 %	1.080 %	- 0.136 %	0.126 %	0.074 %
No.3	0.620 %	0.579 %	0.725 %	- 0.065 %	0.059 %	0.041 %

Subscript Convention and Parameter Definition

X-ray Strain

1=[110], 2=[$\bar{1}$10], 3=[001]

d_{1f} = d-spacing in [110] direction.

d_{2f} = d-spacing in [$\bar{1}$10] direction.

$\varepsilon_1^{xr} = \frac{d_{1f} - d_s}{d_s}$ = mismatch in [110]

$\varepsilon_2^{xr} = \frac{d_{2f} - d_s}{d_s}$ = mismatch in [$\bar{1}$10]

$\varepsilon_3^{xr} = \frac{a_{3f} - a_s}{a_s}$ = in [001]

Elastic Strain

1=[100], 2=[010], 3=[001]

$\varepsilon_1 = \varepsilon_2 = \frac{a_{1f} - a_f}{a_f}$ = compressive

$\varepsilon_3 = \frac{a_{3f} - a_f}{a_f}$ = tensile

$\varepsilon_6 = \psi$ = shear strain

$\varepsilon_f = \frac{a_f - a_s}{a_s}$ = misfit

Table 1. The sample characteristics and x-ray rocking curve results for the MOCVD grown partially relaxed heterojunction epilayers. Also, given are the subscript convention and the definitions of parameters used in the paper.

spacing for all the misfit dislocations projected onto a single ab-plane. These spacings differ by about 7~30 % for the two <110> directions for the samples studied (see Table 1).

The misfit, defined as $\varepsilon_f = (a_f - a_s)/ a_s$ where a_f is the cubic cell lattice constant for the completely relaxed film, can be calculated in a linear elastic theory for the non-equal biaxial stresses along the two <110> directions and zero stress along [001]. In terms of the measured x-ray strains,

$$\varepsilon_f = [\, \nu\, \varepsilon_1^{xr} + \nu\, \varepsilon_2^{xr} + (1-\nu)\, \varepsilon_3^{xr} \,] / (1+\nu) \qquad (2)$$

where ν is the Poisson ratio of the film which is, in terms of the elastic coefficients, $c_{12}/(c_{11} + c_{12})$. The elastic coefficients for a ternary epilayer are obtained from a linear interpolation between the two constituent binary compounds using an estimated ternary composition. The cubic cell lattice constant for the film, a_f, gives the XRC composition for the ternary epilayer through the Vegard's law. The compositions measured this way are listed in Table 1 along with the composition data obtained by EDAX. When the x-ray strains are calculated from the angle separation between the substrate and epilayer peaks as was done here, the composition is a weighted averge over all the GaInAs (epi and buffer) layer thickness. This can introduce error if the layer is graded in composition. More accurate results can be obtained if the dynamical x-ray diffraction theory is used to obtain the x-ray strain depth profile[11]. The composition obtained by EDAX is an average over about 2 μm which is the electron penetration depth in the target material (GaInAs).

The compressive elastic strain is given approximately by $\varepsilon_1 = \varepsilon_2 = 0.5(\, \varepsilon_1^{xr} + \varepsilon_2^{xr}\,) - \varepsilon_f$ for [100] and [010] directions, and the tensile strain by $\varepsilon_3 = \varepsilon_3^{xr} - \varepsilon_f$ for [001] direction. One additional non-zero elastic strain in the partially relaxed film is the shear strain, $\varepsilon_6 = \psi = \varepsilon_1^{xr} - \varepsilon_2^{xr}$, in the (001) plane which comes from the nonequal relaxation for the two <110> directions. The magnitude of the compressive and tensile strains is smaller and the shear strain is greater for a thicker layer without showing any obvious composition-dependence.

3. DISCUSSION

It was recently shown by El-Masry *et al.* that the SLS buffer is extremely effective in blocking the threading dislocations when the local density is low and less effective when the local density is high for a GaAs epilayer on a GaInAs/GaAsP SLS buffer layer grown on a Si substrate[13]. In using the SLS buffer, there need to be enough strained interfaces to bend all the threading dislocations, yet the total SLS thickness remaining under the critical thickness to avoid generating its own dislocations. Also, the average in-plane lattice constant needs to be the same as the epilayer in-plane constant to avoid the misfit dislocations at the SLS-epilayer interface. In our Sample No.1, the In content in the GaInAs layers of the SLS buffer (40 periods of 100Å GaAs + 100Å GaInAs) was twice as much as that in the epilayer. The epilayer in Sample No.1 was free of line defects and cross-hatched patterns even when the layer was etched down by 3~5 μm. This 7 μm thick epilayer is still strained with a comparable elastic strain as other samples. The non-zero elastic strain in Sample No.1 indicates that the surface ridges are not due to the strain state of epilayer but are more likely due to the interface

defects such as misfit dislocations at the buffer-epilayer interface. These interface defect may act as preferred nucleation sites leading to the formation of surface ridges.

The pits on the Nomarski micrograph and the black dots on the topograph for Sample No.1 (Figure 1) are still present when the epilayer is etched down by 3-5 μm. They seem to correspond to threading dislocations with a density of 5000 - 7500 cm^{-2}, which indicate that the SLS buffer in our MOCVD grown sample did not completely block all the threading dislocations and that the threading dislocations are not directly responsible for the surface ridges and the line defects. The graded GaInAs buffer in Sample No.2 does not seem to improve the epilayer quality compared with the plain GaAs buffer of Sample No.3. A cross-section transmission electron microscopy (XTEM) study is necessary to investigate more accurately how effective the graded buffer layer is in reducing defects in the epilayer. Different degree of relaxation for the two <110> directions as manifested in the topographs and Nomarski micrographs is verified by the different in-plane x-ray strains for the two directions. The line defects are more uniformly distributed along one <110> direction compared to the other <110>, which may suggest that different types of dislocations are dominant for each direction. The contrasts or line defects in the x-ray topographs may be images of bundles of these dislocations and they seem to be correlated to the surface ridges. More investigation involving transmission electron microscopy is under way to clarify these aspects and the origins of surface ridges.

In conclusion, the x-ray rocking curve and double crystal topography techniques nondestructively provide many structural characteristics of the partially lattice relaxed epilayers. The topography can also measure the spatial variation of local stress fields when the x-ray beam size is magnified by the first crystal and the local contrast is measured using a densitometer. In this paper, we have shown that the partially relaxed strained epilayer is free of line defects if grown on an SLS buffer layer. An additional unit cell distortion results from the nonequal relaxation along the two <110> directions

4. ACKNOWLEDGMENTS

The work done at SUNY-Buffalo was supported by the National Science Foundation under grant no. ECS-8707111 and by SDI/IST managed by the Office of Naval Research under contract no. N001486K0622. The authors wish to thank Peter Bush at SUNY-Buffalo for the EDAX measurements.

5. REFERENCES

1. K.C. Wang, P.M. Ashbeck, M.F. Chang, G.J. Sullivan, and D.L. Miller, "A 20-GHz frequency divider implemented with heterojunction bipolar transistors," IEEE Trans. Electr. Dev. ED-8(9), 383-385 (1987)

2. D. Feketa, K.T. Chan, J.M. Ballantyne, and L.F. Eastman, "Graded-index separate-confinement InGaAs/GaAs strained-layer quantum well laser grown by metalorganic chemical vapor deposition," Appl. Phys. Lett. 49(24), 1659-1660 (1986)

3. S.M. Liu, M.B. Das, C.K. Peng, J. Klem, T.S. Henderson, W.F. Kopp, and H. Morkoç, "Low-noise behavior of InGaAs quantum-well-structured modulation doped FET's from 10^{-2} to 10^{8} Hz," IEEE Trans. Electr. Dev. ED-33(5), 576-582 (1986)

4. L.P. Ramberg, P.M. Enquist, Y.K. Chen, F.E. Najjar, L.F. Eastman, E.A. Fitzgerald, and K.L. Kavanagh, "Lattice-strained heterojunction InGaAs/GaAs bipolar structures: Recombination properties and device performance," J. Appl. Phys. 61(3), 1234-1236 (1987)

5. S. Kuroda, N. Harada, T. Katakami, and T. Mimura, "HEMT with nonalloyed Ohmic contacts using n^+-InGaAs cap layer," IEEE Elcctr. Dev. Lett. EDL-8(9), 389-391 (1987)

6. E.A. Fitzgerald, D.G. Ast, P.D. Kirchener, G.D. Pettit, and J.M. Woodall, "Structure and recombination in InGaAs/GaAs heterostructures," to be published in J. Appl. Phys. 15 Jan. (1988)

7. G. Burns, C.R. Wie, F.H. Dacol, G.D. Pettit, and J.M. Woodall, "Phonon shifts and strains in strain-layered $(Ga_{1-x}In_x)As$," Appl. Phys. Lett. 51(23), 1919-1921 (1987)

8. C.R. Wie, T.A. Tombrello, and T. Vreeland, Jr., "MeV ion damage in GaAs single crystals: Strain saturation and role of nuclear and electronic collisions in defect production," Phys. Rev. B33(6), 4083-4089 (1986); "MeV ion damage in III-V semiconductors: Saturation and thermal annealing of strain in GaAs and GaP crystals," Nucl. Instr. Meth. B16, 44-49 (1986); C.R. Wie, T. Jones, T.A. Tombrello, T. Vreeland, Jr., F.Xiong, Z. Zhou, G. Burns, and F.H. Dacol, "Radiation defect-induced lattice contraction of InP", Matr. Res. Soc. Symp. Proc. 74, 517-522 (1987)

9. C.R. Wie, "Defect strain fields in epitaxial GaAs," B24/25, 562-564 (1987)

10. C.R. Wie, K. Xie, G. Burns, F.H. Dacol, G.D. Pettit, and J.M. Woodall, "X-ray and Raman studies of MeV ion implanted GaInAs/GaAs," Matr. Res. Soc. Symp. Proc. E104 (1988), in press.

11. C.R. Wie, T.A. Tombrello, and T. Vreeland, Jr., "Dynamical x-ray diffraction from nonuniform crystalline films: Application to x-ray rocking curve analysis," J. Appl. Phys. 59(11), 3743-3746 (1986)

12. I.J. Fritz, P.L. Gourley, and L.R. Dawson, "Critical layer thickness in $In_{.2}Ga_{.8}As$/GaAs single strained quantum well structures," Appl. Phys. Lett. 51(13), 1004-1006 (1987)

13. N. El-Masry, J.C.L. Tarn, T.P. Humphreys, N. Hamaguchi, N.H. Karam, and S.M. Bedair, "Effectiveness of strained-layer superlattices in reducing defects in GaAs epilayers grown on silicon substrates," Appl. Phys. Lett. 51(20), 1608-1610 (1987).